Received 20 December 2024; revised 18 January 2025; accepted 6 February 2025. Date of publication 13 February 2025; date of current version 28 February 2025.

Digital Object Identifier 10.1109/OJCOMS.2025.3541962

Handover Strategy for LEO Satellite Networks Using Bipartite Graph and Hysteresis Margin

SAHAR EYDIAN, MARYAM HOSSEINI, AND GUNES KARABULUT KURT (Senior Member, IEEE)

Poly-Grames Research Center, Department of Electrical Engineering, Polytechnique Montréal, Montréal, QC H3C 3A7, Canada

CORRESPONDING AUTHOR: S. EYDIAN (e-mail: sahar.eydian@polymtl.ca)

This work was supported in part by the Tier 1 Canada Research Chair Program.

ABSTRACT The low Earth orbit (LEO) satellite constellation has become a highly effective solution for non-terrestrial networks (NTN), offering reliable, uninterrupted, and high-speed global communication. However, the rapid movement of LEO satellites results in a significant handover rate across satellites. Therefore, satellite handover management is essential to ensure the stability and continuity of communication services. This paper proposes a novel weighted bipartite graph-based handover strategy in LEO constellations to enhance quality of service (QoS) and overcome the challenge of frequent satellite handovers. The proposed approach utilizes the Kuhn-Munkres (KM) algorithm to achieve optimal matching with maximum weight, thereby ensuring efficient load distribution and high-quality communication. Moreover, the implementation of hysteresis margin (HM) reduces unnecessary handovers and thus enhances the overall performance of the network. The numerical results demonstrate a significant reduction in handover rate and latency, while improving energy efficiency and achieving enhanced data rates. In particular, our scheme effectively adapts to varying Rician K-factors and demonstrates flexibility under different signal conditions. Furthermore, the obtained results highlight a significant reduction in handover costs and ensure efficient and reliable communication in LEO satellite networks.

INDEX TERMS Low earth orbit, satellite handover, weighted bipartite graph, maximum weight matching, hysteresis margin.

I. INTRODUCTION

SATELLITE communications play an important role in providing seamless global connectivity and overcoming the inherent limitations of terrestrial mobile communications. The low Earth orbit (LEO) constellations, with orbits deployed at altitudes between 500 km and 1500 km, allow lower transmission latency and higher throughput compared to geostationary earth orbit (GEO) satellites [1]. Furthermore, the low altitude of the satellites reduces power requirements and minimizes signal attenuation, which is critical to reducing the size of ground equipment [2]. In recent years, the demand for broadband services offered by large constellations of LEO satellite networks (e.g., Kuiper, Starlink, OneWeb, and Lightspeed) has increased. For example, Starlink provides low-latency (i.e., below 30 ms), high-data-rate (i.e., above 100 Mb/s) satellite broadband services to inaccessible areas [3], [4]. Therefore, the LEO constellation will be a key component in the evolution of communication systems.

Although LEO communication system deployments offer unique advantages, these systems are characterized by high mobility. Their footprints can change with velocities of 7.56 km/s [5], completes one orbit around the Earth in about 100 minutes [6]. Therefore, each satellite can serve the gateway stations for a limited time, which is usually shorter than the duration of a connection [7]. To ensure uninterrupted communication, once the current satellite is no longer able to provide services to the gateway station, it is necessary to handover the communication link to another visible satellite. The rapid motion of LEO satellites causes constant changes in constellation topology, resulting in frequent handovers and significantly affects quality of service (QoS).

Moreover, the gateway stations are often covered by several satellites simultaneously, allowing them to leverage satellite diversity to select optimal handover targets [9]. However, the large signal propagation distance between the satellite and the ground results in smaller variations in received signal strength (RSS) compared to terrestrial

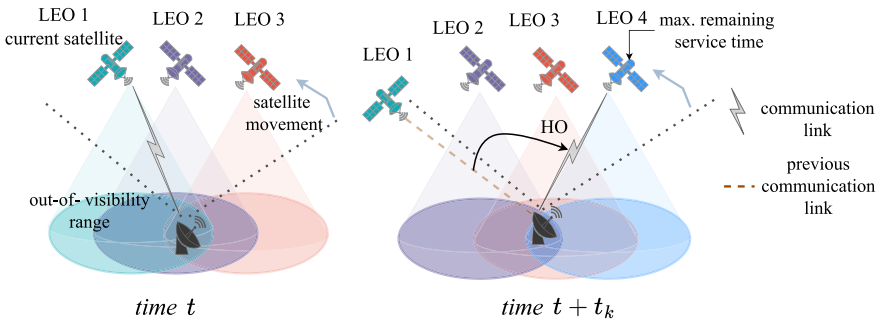

FIGURE 1. Illustration of successive moments t and $t + t_k$, during which a handover is performed based on the maximum visibility of satellite.

networks (TNs) [10]. Directly mirroring handover mechanisms from TNs to non-terrestrial networks (NTN) may limit the gateway station's ability to identify optimal targets [11], [12]. In addition, satellite handover can present several challenges, including latency, path loss, and signal overhead [13], [32]. Therefore, designing an effective satellite handover scheme is crucial to reducing the frequency of handovers, balancing satellite load, and ensuring high communication quality.

Various satellite handover approaches have been proposed in the literature utilizing decision criteria such as elevation angle [14], [15], [42], maximum service time (MST) [16], [17], [18], [19], [20], [21], [27], maximum number of idle satellites [15], [22], [23], [24], delay [25], [26], [27], handover failure [22], [23], [28], and load, etc. The strategies that rely on MST and utilize ephemeris data to measure service time are efforts to significantly reduce handover times, delays, and signaling costs. This strategy evaluates the remaining service time of candidate satellites prior to the handover. As illustrated in Fig. 1, at the handover time $t + t_k$, the communication link is handed over to candidate LEO 4, which offers the maximum remaining service time among the available options. However, it may result in an unbalanced distribution of satellite loads and decrease channel quality [34].

The authors in [16] introduced a velocity-aware handover prediction technique to identify target satellites with maximum service duration. While this method reduces handover rates and failure probabilities, it overlooks network quality, compromising the ability to ensure QoS for users. Similarly, strategies that prioritize idle satellite channels or elevation angles may increase handover events and overload specific satellites, compromising QoS [29], [33]. These limitations highlight the need for more intelligent, multi-attribute approaches that prioritize dynamic factors such as channel quality and handover rate to enhance handover decisions and improve overall communication stability.

A. RELATED WORK

Several methods were developed and implemented to improve the mentioned metrics in satellite handover, each focusing on different aspects of performance. An overview of these methods is presented in Table 1.

TABLE 1. Overview of satellite HO methods.

Method	Reference
Graph theory	[14], [16], [30], [36], [39], [40], [42], [49]
Learning algorithm	[17], [18], [23], [28], [50]
Architecture design	[25], [26], [31]
Handover schemes design	[24]
Decision technique	[19], [21], [22]
Game theory	[42]

Decision-based techniques, such as the real-time handover method proposed in [21], leverage global positioning system (GPS) to minimize handovers by predicting largest service time. However, these approaches may lead to unbalanced satellite loads and compromised QoS.

Reinforcement learning based methods have shown promise for enhancing satellite handovers. In [17], a quality of experience (QoE) driven algorithm optimizes handovers by considering service time and channel resources, significantly improving success rates and minimizing disruptions. Similarly, [50] introduced a Nash Soft Actor-Critic (NSAC) algorithm for high-mobility scenarios, modeling handovers as a Nash equilibrium problem to enhance success rates, reduce latency, and balance load.

Graph-based methods are another prominent category. In [36], a weighted bipartite graph framework was developed to optimize decisions based on channel quality, service time, and system load, reducing handover failures. The study in [14] proposes a dynamic handover framework for LEO and TNs using a multi-attribute graph and the Floyd algorithm to optimize handover paths, minimize delays, and enhance QoS. Similarly, [30] combines a genetic algorithm with a multi-attribute graph to optimize handover paths, improving both network efficiency and QoS. In [42], a game-theoretical model combined with a bipartite graph in a software-defined satellite network architecture is proposed to optimize resource allocation and minimize handover delays. This approach, tested on the Iridium network, reduces call drops and balances network load, improving overall communication reliability.

The authors in [40] present a handover management strategy for LEO satellite networks using a weighted bipartite graph and a maximum weight matching (MWM) solution

to achieve high communication quality and efficient load balancing. This approach integrates multiple-input multiple-output (MIMO) technology to enhance data rates and overall performance but overlooks the challenge of frequent handovers, which increase operational costs and degrade QoS. Similarly, [39] proposes a directed graph framework to minimize handover numbers and improve data rates by incorporating criteria like elevation angle and service time into the graph's edge weights, optimized using a shortest-path algorithm. However, its reliance on elevation angle as the primary indicator of link quality can result in suboptimal decisions. In our study, we compare these two methods alongside the MST strategy, addressing their limitations by prioritizing channel quality, balancing load, reducing frequent handovers, and improving stability. These baselines were chosen to reflect key approaches in satellite handover strategies: maximizing data rate (MWM strategy), minimizing handover rate (MST startegy), and considering both metrics (Shortest Path strategy).

Moreover, existing satellite handover strategies often rely on multiple criteria, such as channel quality, service time, and available channels, to manage mobility and handover decisions. While effective in specific scenarios, these methods may introduce complexity and may not consistently achieve a balance across all desired outcomes. A significant trade-off persists between data rate and handover frequency, where improving one often adversely impacts the other. Balancing this trade-off remains a key challenge in developing effective LEO satellite handover strategies. Building on the strengths and addressing the limitations of existing methods, this study proposes an effective LEO satellite handover approach.

To address the limitations, we propose a flexible and efficient handover management strategy using a weighted bipartite graph framework. This framework effectively models the dynamic interactions between LEO satellites and gateway stations, enabling structured handover decisions at each time slot. By employing the Kuhn-Munkres (KM) algorithm, the strategy achieves MWM, ensuring high-quality links, efficient load distribution, and minimized resource conflicts—key to maintaining QoS in LEO networks. For instance, in Starlink-like constellations, the KM algorithm's computational efficiency supports dynamic gateway coverage and enhances performance under varying network conditions. Furthermore, proposed method prioritizes channel gain as the primary criterion, streamlining decision-making.

To enhance stability and reduce frequent handovers, we integrate a hysteresis margin (HM) mechanism into our framework and KM algorithm. This integration addresses key challenges in LEO satellite networks by extending connection duration when link quality is acceptable, thereby minimizing unnecessary handovers without compromising data rates. This mechanism enables operators to dynamically adjust priorities among latency, stability, and throughput, ensuring adaptability to fluctuating network conditions. Additionally, the strategy's robustness and flexibility are demonstrated under varying Rician K-factor conditions, highlighting its effectiveness across different network scenarios. The primary objectives of this study are to reduce handover frequency, improve data rates, and achieve efficient load balancing.

B. CONTRIBUTIONS AND ORGANIZATION

The main contributions of this paper can be summarized as follows:

- The dynamic interactions between LEO satellites and gateway stations are modeled as a weighted bipartite graph, where vertices represent satellites and gateway stations, and edges are weighted by channel gain, reflecting real-time communication quality. Unlike shortest path strategy that rely on elevation angle, our method prioritizes actual channel quality for handover decisions, achieving higher data rates and improved performance under varying network conditions.
- The KM algorithm is employed to achieve MWM, ensuring high-quality connections and efficient load distribution. By preventing multiple gateway stations from selecting the same satellite as the switching target during handovers, this approach improves network performance and minimizes congestion risks.
- To reduce frequent handovers and enhance network stability, a HM mechanism is integrated into the KM algorithm and handover selection process. The proposed method achieves handover rates comparable to the MST strategy while enhancing data rates similar to the MWM strategy. By effectively balancing these objectives, it addresses the limitations of both strategies without sacrificing one for the other. Although the inherent trade-off between data rate and handover rate is not fully eliminated, the method provides a stable and efficient solution to key challenges in dynamic LEO satellite networks, paving the way for future optimization.
- The proposed handover strategy reduces latency compared to conventional methods, ensuring enhanced performance for delay-sensitive applications, while achieving energy efficiency comparable to the MWM strategy. This demonstrates its ability to balance energy consumption while maintaining handover stability and communication quality.
- The adjustable HM mechanism provides flexibility to meet varying regional demands, technological requirements, and operator priorities. By enabling adjustments for higher data rates or lower latency, it ensures adaptability to different network conditions. Additionally, the reduced handover frequency in the proposed strategy contributes to lower operational and handover costs, offering practical benefits for network operators.

The rest of this letter is structured as follows: Section II presents the system model based on a bipartite graph. The proposed scheme is detailed in Section III. In Section IV, the performance of the proposed scheme is theoretically analyzed. Section V presents the framework evaluation to

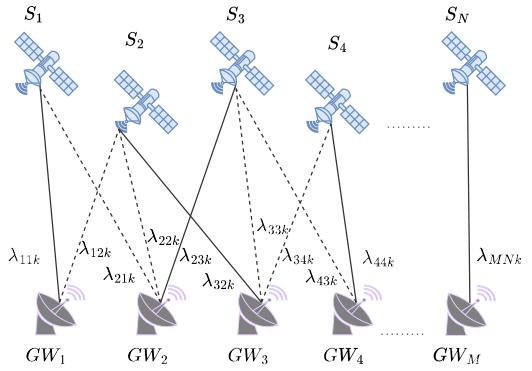

FIGURE 2. System model showing the connections of LEO satellites and gateway stations. Here, S_j denotes the j-th LEO satellite where $j = 1, 2, \ldots, N$. GW_i denotes the i-th gateway station where $i = 1, 2, \ldots, M$. λ_{ijk} represents the weight of the communication link between the i-th gateway station and the j-th LEO satellite at time slot t_k.

demonstrate the efficacy of the proposed method. Finally, the findings of the conclusion are given in Section VI.

II. SYSTEM MODEL

A. NETWORK MODEL

The relationship and connection among LEO satellites and gateway stations can be represented as a bipartite graph as illustrated in Fig. 2.

We consider the downlink of an LEO satellite network that includes a total of N LEO satellites, and the S_j indicates the j-th LEO satellite, where $j = 1, 2, \ldots, N$. Similarly, the model contains the total of M gateway stations, and GW_i indicate the i-th gateway station, where $i = 1, 2, \ldots, M$. The corresponding weight for the communication link at time slot t_k between GW_i and S_j is λ_{ijk}. The frequently used notations are summarized in Table 2.

The gateway stations' positions are represented using geodetic coordinates in the world geodetic system (WGS 84), which serves as the standard reference ellipsoid for the GPS. Thus, the location of each gateway station is specified by the tuple $(\text{Lat}_i, \text{Lon}_i, \text{Alt}_i)$, where the latitude is within the range of $[-90°, 90°]$, the longitude ranges from $[-180°, 180°]$, and the altitude is measured in meters [12].

The satellite orbits are determined using publicly available two-line element (TLE) data, sourced from platforms like *NORAD* and *CelesTrak*. TLE data includes essential orbital parameters, such as inclination, eccentricity, right ascension of the ascending node (RAAN), and true anomaly, which define the satellite's trajectory and position over time [48]. These parameters enable precise predictions of satellite positions relative to the gateway stations at any given moment. The TLE files are regularly updated to ensure accuracy in satellite trajectory forecasts.

B. CHANNEL MODEL

The channel model is influenced by two main types of fading: large-scale and small-scale fading, each caused by different factors. Large-scale fading primarily results from free-space path loss and additional attenuation due to atmospheric conditions, such as weather and atmospheric particles. On the other hand, small-scale fading is primarily characterized by Rician fading, which results from the direct line-of-sight (LoS) connections between satellites and ground stations in satellite communication systems. The channel model expression mainly consists of path loss, atmospheric fading, and Rician small-scale fading [36], which expressed as follows

$$G_{ijk} = \left(\frac{c_{\text{light}}}{4\pi d_{ijk} f_c}\right)^2 A(d)\varphi_{ijk}, \tag{1}$$

where c_{light} is the speed of light and f_c is the carrier frequency. d is the distance between satellites and the gateway station, φ_{ijk} represents the Rician small-scale fading, and $A(d)$ is related to the atmospheric fading due to clouds and rain, which can be given by [37]

$$A(d) = 10^{\frac{3d\chi}{10h}}, \tag{2}$$

where χ is the attenuation through the clouds and rain in dB/km. Moreover, d is the propagation distance between the satellite and the gateway station, and h is satellite altitude.

The small scale fading is modeled as Rician fading since the links consist of both LoS and non-line-of-sight (NLoS) components. The probability of having a strong

TABLE 2. Frequently used notations.

Notation	Description
N	Total number of satellites
M	Total number of gateway stations
S_j	j-th satellite
GW_i	i-th gateway station
λ_{ijk}	Link weight between GW_i and S_j at t_k
t_{ij}^{in}	Time when S_j enters the coverage area of GW_i
t_{ij}^{out}	Time when S_j leaves the coverage area of GW_i
t_k	The k-th time slot in duration time of T
G_{ijk}	Channel gain between GW_i and S_j at time t_k
F_H	Hysteresis coefficient
H	Hysteresis margin
c_{light}	Speed of light
f_c	Carrier frequency
d_{ijk}	Distance between S_j and GW_i at time t_k
$A(d)$	Atmospheric fading as a function of distance d
φ_{ijk}	Small-scale fading component, modeled as Rician
σ	Large value of hysteresis coefficient
χ	Attenuation through the clouds and rain
K_{ijk}	Rician K-factor between GW_i and S_j at t_k
ϕ_{ijk}	Phase related to LoS component for GW_i and S_j at t_k
$\mathcal{F}_k$	Set of matching elements at time t_{k-1}
$G_{ij}^{'}$	Initial channel gain between GW_i and S_j
$\mathcal{G}(:,:,k)$	Matrix representation of S_j and GW_i at time t_k
$\mathcal{G}'(:,:,k)$	Adjusted matrix of S_j and GW_i at time t_k
$\mathcal{M}(:,:,k)$	Matching matrix derived via KM algorithm at t_k
w_{ijk}	Link weight between GW_i and S_j at t_k in $\mathcal{M}(i,j,k)$
$\{i,j,k\}$	Selected S_j for GW_i in matching matrix $\mathcal{M}(i,j,k)$
(i,j,k)	Candidate S_j for GW_i in matrix $\mathcal{G}(i,j,k)$

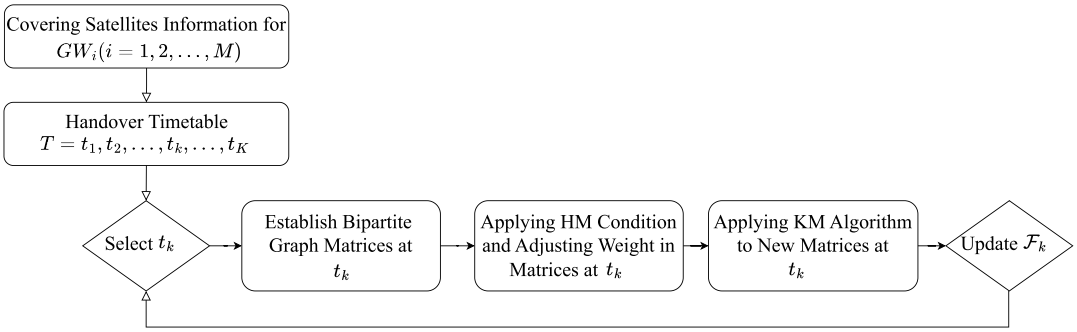

FIGURE 3. Overview of the Proposed Handover Decision Process.

LoS component increases with the elevation angle, reaching its maximum when the satellite is directly overhead (90° elevation).

For the purpose of modeling, it is assumed that the channel conditions remain constant over a coherence time interval τ_c, thus allowing the use of a flat fading (non-frequency selective) model. This assumption simplifies analysis by ensuring that the fading uniformly affects the entire bandwidth, which is valid when the coherence bandwidth exceeds the signal bandwidth.

The Rician fading channel gain, φ_{ijk}, is expressed as follows [48]

$$\varphi_{ijk} = \sqrt{\frac{K_{ijk}}{K_{ijk}+1}} e^{j\phi_{ijk}} + \sqrt{\frac{1}{K_{ijk}+1}} h_{ijk}^{\text{NLoS}}, \tag{3}$$

where

- K_{ijk} is the Rician K-factor, representing the ratio of the power of the direct LoS path to that of the scattered NLoS components.
- ϕ_{ijk} is the phase associated with the LoS component, uniformly distributed as $\phi_{ijk} \sim \mathcal{U}[-\pi, \pi]$.
- $h_{ijk}^{\text{NLoS}} \sim \mathcal{CN}(0, 1)$ represents the Rayleigh fading component, modeling the NLoS multipath scattering.

The first term of equation (3) corresponds to the deterministic LoS component, while the second term models the stochastic NLoS scattering. The Rician K-factor K_{ijk} is crucial for characterizing the relative strength of the LoS and NLoS components, with higher K-values indicating stronger LoS paths and lower K-values reflecting a greater influence of NLoS scattering.

III. PROPOSED SCHEME

This section outlines a handover management strategy for LEO satellite networks. The proposed scheme addresses the challenges of frequent handovers, load balancing, and communication quality in dynamic satellite networks. Each subsection describes a specific component, detailing its purpose, methodology, and role in the overall framework.

Fig. 3 provides an overview of the proposed handover decision process. First, the covering satellite information for each gateway station is obtained, and a handover timetable is constructed. For each time slot, the satellites visible to the gateway stations are modeled as a bipartite graph. The algorithm calculates the selected satellites for the gateway stations using the HM mechanism and MWM methods and updates the results. These results are fed back into the algorithm to adjust weights for the next time slot based on historical information and real-time conditions, ensuring continuity and stability in the handover process.

A. ESTABLISHING BIPARTITE GRAPH

Managing handover decisions in dynamic LEO satellite networks requires an accurate representation of the interactions between gateway stations and satellites. A bipartite graph provides a structured framework to model these interactions, capturing time-dependent connectivity and supporting efficient decision-making under variable satellite coverage. This subsection introduces the establishment of bipartite graph matrices, which reflect the visibility and communication link status between gateway stations and satellites.

Given the predictability of the LEO satellite's trajectory, the gateway station can identify and get information on the satellites passing within its visibility range using the methodology suggested in [41]. The coverage information for the satellites passing over gateway station GW_i can be expressed as follows

$$Coverage\ Table\ GW_i = \begin{bmatrix} S_1 & S_2 & S_3 & \ldots & S_N \\ t_{i1}^{in} & t_{i2}^{in} & t_{i3}^{in} & \ldots & t_{iN}^{in} \\ t_{i1}^{out} & t_{i2}^{out} & t_{i3}^{out} & \ldots & t_{iN}^{out} \end{bmatrix}, \tag{4}$$

where the first row represents the indices of the covering satellites, the second row indicates the enter time of satellite S_j to the visibility range of gateway station GW_i by the element t_{ij}^{in}, and the third row indicates the leave time of satellite S_j from the visibility range of gateway station GW_i by the element t_{ij}^{out}. To prevent disruptions to ongoing communications, the gateway station shifts to an alternative satellite upon exiting the current serving satellite's coverage area.

The assumption is that handover may occur when a satellite enters or exits the gateway station view range. For gateway stations to maintain connectivity with certain QoS requirements, a handover sequence among the passing

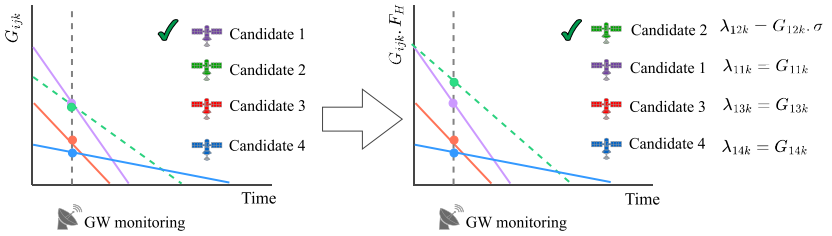

FIGURE 4. Change in monitoring condition for gateway station.

satellites is required for a time period, T. Let us assume that T is divided to K time slots, where the kth time slot in T is represented by $t_k \in T = [t_1, t_2, \ldots, t_k, \ldots, t_K]$. Hence, the ground station can uniformly manage the access and handovers of the gateway station.

As shown in Fig. 2, from the perspective of the gateway station, at a given time, there is often more than one satellite available to access simultaneously. In this figure, solid lines indicate active connections between the gateway stations and satellites, while dotted lines indicate potential connections to candidate satellites. These indicate that although the satellite can provide services to the gateway stations, might not be best candidate at the moment. To establish a bipartite graph for each time slot t_k, focusing on the communication status between each satellite S_j and gateway station GW_i, the following analysis should be considered

- If $t_{ij}^{in} \leq t_k < t_{ij}^{out}$, then S_j is within the visibility range of GW_i, indicating that GW_i can select S_j at t_k.
- If $t_k < t_{ij}^{in}$ or $t_k \geq t_{ij}^{out}$, then S_j is outside the visibility range of GW_i, indicating that S_j is not a candidate satellite for GW_i at t_k.

Based on these conditions, the initial bigraph matrices, denoted by $\mathcal{G}(, :, k)$, that reflects the communication link status between GW_i and S_j at time t_k defined as follows

$$\mathcal{G}(i,j,k) = \begin{array}{c} \\ GW_1 \\ GW_2 \\ \vdots \\ GW_M \end{array} \begin{array}{c} \begin{array}{cccc} S_1 & S_2 & \ldots & S_N \end{array} \\ \begin{bmatrix} \lambda_{11k} & \lambda_{12k} & \ldots & \lambda_{1Nk} \\ \lambda_{21k} & \lambda_{22k} & \ldots & \lambda_{2Nk} \\ \vdots & \vdots & \ddots & \vdots \\ \lambda_{M1k} & \lambda_{M2k} & \ldots & \lambda_{MNk} \end{bmatrix} \end{array}, \tag{5}$$

where each array represents the weight of the communication link between each satellite and the corresponding gateway station at t_k. The λ_{ijk}, which represents the weight of the communication link between GW_i and S_j at time slot t_k, can be determined according to the following rule

$$\mathcal{G}(i,j,k) = \lambda_{ijk}, \begin{cases} \lambda_{ijk} > 0, \text{ if } t_{ij}^{in} \leq t_k < t_{ij}^{out} \\ \lambda_{ijk} = 0, \text{ if } t_k < t_{ij}^{in} \text{ or } t_k \geq t_{ij}^{out}. \end{cases} \tag{6}$$

In case $\lambda_{ijk} > 0$, then S_j becomes a possible candidate for handover to GW_i during time slot t_k. Otherwise, in case $\lambda_{ijk} = 0$, then S_j cannot be considered as a potential handover candidate for GW_i at t_k. Therefore, the sequence of bipartite graph matrices for each time slot from t_1 through to t_k can be generated and represented as $\mathcal{G}(:, :, k)$ where $k \in \{1, \ldots, K\}$. The bipartite graph provides a dynamic representation of satellite-gateway interactions, forming the foundation for the subsequent steps in the proposed scheme.

B. WEIGHT CONFIGURATION

This subsection introduces a weight configuration process for communication links between satellites and gateway stations. By integrating channel gain and a HM mechanism, the method accurately reflects service quality and stability, ensuring effective handover decisions in dynamic LEO networks.

Due to the competitive nature of satellite handover, using a binary link weight of 1 or 0 in the bipartite graph framework [42] fails to accurately describe the difference in channel quality. To address this, we utilize channel gain G_{ijk} as the primary weight component to reflect different levels of service quality across channels. However, relying only on channel gain leads to unnecessary handovers, as the gateway stations must quickly switch to another visible satellites if the selected satellite has a short service time. In addition, frequent handovers lead to service disruptions, reduced network efficiency, a lower user experience, more signalling overhead, and increased handover costs. Fig. 4 illustrates the evaluation process of a gateway station for various candidate satellites before conditional handover event.

At the time t_k under multi-coverage, each candidate's gain G_{ijk} can be obtained using equation (1) and through ephemeris data. Typically, the gateway station selects the candidate with the greatest G_{ijk}, as shown on the left side of Fig. 4. It is obvious that candidate 1 provides the highest G_{ijk} and makes it the preferred option. However, if candidate 1 has a short service duration, the gateway station must quickly switch to an alternative candidate, which increases the handover rate and an interruption in service continuity. Therefore, we introduce HM as the second weight component to improve handover decisions. The configuration of λ_{ijk} is represented as follows

$$\lambda_{ijk} = G_{ijk} \times F_H, \tag{7}$$

where G_{ijk} represents the channel gain between GW_i and S_j at time instant t_k and reflects the link quality. Moreover, F_H denotes the hysteresis coefficient between GW_i and S_j at time slot t_k and is responsible for keeping connectivity to the satellites as long as they provide high-quality services.

The F_H is a factor that controls the handover decision process and decreases frequent handovers. The value of F_H is determined by HM condition. Specifically:

$$F_H = \begin{cases} \sigma, \text{ if } S_j \text{ satisfies HM condition for } GW_i, \\ 1, \text{ if } S_j \text{ does not satisfy HM condition for } GW_i, \end{cases} \tag{8}$$

where σ is a large constant value (set to 10 dB) that increases the weight of a link when the HM condition is satisfied. Specifically, if a satellite satisfies the HM condition—meaning its link quality exceeds a predefined threshold—F_H is set to σ. This ensures that the satellite with a stable connection is prioritized during the handover process, even if other candidates have slightly higher channel gains initially. In contrast, if the HM condition is not met, F_H remains 1, and the handover decision is made based solely on the channel gain G_{ijk}. As shown in Fig. 4, the weight of Candidate 2 is increased to $G_{12k} \times \sigma$, allowing it to be prioritized over Candidate 1, which has a higher initial link gain. This method effectively balances reducing handover frequency and maintaining high-quality communication by prioritizing satellites that ensure stable connections. It also ensures fairness and stability in the network's resource allocation by avoiding excessive handovers while improving overall link quality.

The weight configuration balances link quality and handover frequency, setting the stage for efficient and stable handover decisions.

C. WEIGHT ADJUSTMENT

Dynamic weight adjustment based on real-time conditions is essential for effective handover management. This subsection introduces a process that leverages historical data to refine link weights and prepares them for the application of HM conditions.

Given the obtained matrices $\mathcal{G}(:,:,k)$, we have the information of satellites coverage for each gateway station from t_1 to t_k. For convenience, we define each candidate S_j for a certain GW_i at $\mathcal{G}(i,j,k)$ as potential matching elements and represent with $\{i,j,k\}$. Subsequently, we define the selected S_j for a certain GW_i as a matching elements and represent with (i,j,k). In addition, we employ the set $\mathcal{F}_k$ to store the network state at each time slot, including the information of matching elements, with their corresponding initial channel gains.

Based on the proposed method, we aim to select the satellite with the highest service quality for the maximum possible time. This intelligent strategy evaluates whether the matching elements at time slot t_{k-1} remain as qualified candidates at the instant t_k. This step ensures that we consider the past condition of the system, thereby adding a layer of continuity to the selection process. To this end, the proposed scheme verifies the presence of any potential matching elements $\{i,j,k\}$ in set $\mathcal{F}_k$, which may have the following results

- For those $\{i,j,k\}$ found in set $\mathcal{F}_k$, meaning that S_j has continued coverage from handover time t_{k-1} till t_{k+1} for corresponding GW_i.
- For those $\{i,j,k\}$ not found in set $\mathcal{F}_k$, meaning that S_j did not have coverage or was not the best candidate for the corresponding GW_i during time slot t_{k-1}.

Based on the above discussion, weight adjustment in bipartite graph matrices $\mathcal{G}(:,:,k)$ can be represented as follows

$$\mathcal{G}(i,j,k) \ = \lambda_{ijk}, \begin{cases} \{i,j,k\} \ \in \mathcal{F}_k, \ \text{then } \lambda_{ijk} = G_{ijk} \times F_H \\ \{i,j,k\} \ \notin \mathcal{F}_k, \ \text{then } \lambda_{ijk} = G_{ijk}. \end{cases} \tag{9}$$

In the first condition, integrating an HM into the handover mechanism significantly enhances the performance of the selection scheme by introducing a suitable criterion for service stability. Consequently, the value of λ_{ijk} depends on the HM conditions. In the second condition, the serving satellite S_j at t_{k-1} has been finished it's coverage on GW_i, and hence we consider $\mathcal{F}_k$ equal to 1 in the function λ_{ijk}.

The weight adjustment process refines link selection by integrating historical data, ensuring the system is prepared for applying HM conditions in the next step.

D. HYSTERESIS MARGIN AND ALGORITHM ENHANCEMENT

Frequent handovers disrupt communication quality and elevate operational costs. This subsection introduces the application of the HM condition, which adjusts weights to create updated matrices that prioritize stable connections while maintaining link quality.

To investigate the HM condition for those $\{i,j,k\}$ found in set $\mathcal{F}_k$, the proposed method compares the current channel quality of the $\{i,j,k\}$ with its initial value at t_k to adjust the weight and achieve the new bipartite matrix $\mathcal{G}'(:,:,k)$. Therefore, by applying the HM condition, the weight in $\mathcal{G}(:,:,k)$ can be adjusted and expressed as a new matrix $\mathcal{G}'(:,:,k)$ as follows

$$\mathcal{G}'(i,j,k) \ = \lambda'_{ijk}, \begin{cases} \lambda'_{ijk} = G_{ijk} \times F_H, \quad \text{where } F_H = \sigma, \\ \quad \forall \{i,j,k\} \in F_k \wedge G_{ijk} \geq G'_{ij} + H, \\ \lambda'_{ijk} = G_{ijk} \times F_H, \quad \text{where } F_H = 1, \\ \quad \forall \{i,j,k\} \in F_k \wedge G_{ijk} < G'_{ij} + H, \\ \lambda'_{ijk} = G_{ijk}, \\ \quad \forall \{i,j,k\} \notin F_k, \end{cases} \tag{10}$$

represents the updated weight of the communication link between GW_i and S_j at time slot t_k, incorporating the HM condition. G'_{ij} represents the channel gain between GW_i and S_j at the first time, H is the hysteresis margin, and σ is a large value for F_H.

In the first case, the proposed algorithm evaluates the handover margin condition. If S_j satisfies the specified requirements for the corresponding GW_i, it can be considered qualified to continue providing service for GW_i among other candidate satellites. Therefore, the proposed scheme effectively prevents frequent handover while ensuring a high-quality connection by maintaining S_j for GW_i at time slot t_k. To this end, we increase the link weight by multiplying a large hysteresis coefficient, σ, in G_{ijk} at $\mathcal{G}'(i,j,k)$. This strategic adjustment prioritizes S_j as the preferred handover

candidate for GW_i at t_k, thus emphasizing service reliability above temporary quality improvements. In contrast, if S_j fails to satisfy the HM condition for the corresponding GW_i, it implies that S_j may not provide high-quality service to GW_i compared to other candidate satellites. As a result, GW_i may needs to identify a qualified alternative satellite at t_k, thereby the algorithm assigns the default weight G_{ijk} to $\mathcal{G}'(i,j,k)$.

In the second case, since the coverage of serving satellite S_j for GW_i at t_{k-1} has ended at t_k, GW_i must switch to other satellites. Thus, we assign G_{ijk} as the weight in $\mathcal{G}'(i,j,k)$ to find the best target satellite for GW_i at t_k. The HM mechanism reduces unnecessary handovers and enhances network stability, making it a crucial component of the proposed scheme.

E. MAXIMUM WEIGHT MATCHING

In this subsection, a MWM approach is employed to achieve high-quality links and balanced load distribution. This design addresses resource conflicts and enhances overall communication quality.

The rapid expansion in communication demands, which results from ever-increasing communication terminals, creates significant pressure on satellite resources. Therefore, to prevent resource wastage and overloading, it is essential to not only maintain high-quality links but also ensure that the operational load is uniformly distributed among satellites. With the bigraph matrices $\mathcal{G}'(:,:,k)$ developed for each time slot from t_1 to t_K, our objective is to achieve high link quality with balanced load distribution across the satellite network.

Within this particular scenario, the concept of matching within a bipartite graph becomes essential. This graph defines a match as a subset of edges where no two edges share a common vertex. The objective of the MWM is to identify a pairing that maximizes the total weight of the edges included in the matching. This method with KM algorithm is particularly well-suited for our system model, which prioritizes load balancing and link quality. Given a complete weighted bipartite graph $\mathcal{G}'(i,j,k)$, the goal of the KM algorithm is to find a matching $\mathcal{M}$ that maximizes the total weight, defined as

$$w(\mathcal{M}) = \sum_{(i,j)\in\mathcal{M}} \lambda'_{ijk}. \tag{11}$$

This matching improves communication link quality and load balancing between gateway stations and satellites. By utilizing the KM technique to our weighted bigraph $\mathcal{G}'(:,:,k)$, we derive the matching matrices, represented as $\mathcal{M}(:,:,k)$. The outcome matching matrices $\mathcal{M}(:,:,k)$ from KM algorithm, is defined as

$$\mathcal{M}(i,j,k) = w_{ijk}, \begin{cases} w_{ijk} = \lambda'_{ijk}, & \text{if } GW_i \text{ matches } S_j \\ w_{ijk} = 0, & \text{if } GW_i \text{ does not match } S_j. \end{cases} \tag{12}$$

The proposed method and the handover decision process are depicted in Algorithm 1.

The KM algorithm maximizes the sum of weights in the matching matrix $\mathcal{M}(:,:,k)$, selects the best link quality for each gateway station, and reduces the handover number by integrating HM. By consistently implementing the KM method for each time slot, we ensure that each gateway station matches the satellite with the highest link quality based on the latest data. The proposed method also facilitates the efficient use of satellite resources and significantly reduces the handover rate. Finally, the outcomes derived from the KM method are stored in $\mathcal{F}_k$ to be utilized in the subsequent time slot. The MWM process enhances link quality and load distribution, effectively addressing key challenges in dynamic LEO satellite networks.

Algorithm 1 Proposed Satellite Handover Decision Process

```
Initialize satellites coverage S_j for gateway GW_i.
Initialize H and F_H.
Define and initialize set F_k.
for all time slots k in T, k = 1, 2, ..., K do
    Establish initial bipartite matrices G(:, :, k).
    Weight adjustment operation:
    for all {i, j, k} in G(:, :, k) do
        if {i, j, k} is found in F_k then
            Check HM condition
            if HM condition is met then
                Increase the weight of {i, j, k} using (6).
                Adjust the weight in G'(:, :, k).
                Handover does not occur.
            else
                Assign G_ijk as weight in G'(:, :, k).
            end if
        else
            Assign G_ijk as the weight of in G'(:, :, k)
        end if
    end for
    Compute M(:, :, k) using the KM to G'(:, :, k)
    Update F_k with the results from M(:, :, k) for the
next time slot.
end for
```

IV. PERFORMANCE ANALYSIS OF THE PROPOSED SCHEME

A. AVERAGE DATA RATE

The received power, denoted by $P_{rx,k}$, is crucial for calculating data rates. $P_{rx,k}$ is defined as [37]

$$P_{rx,k} = P_{tx,k} \times G_{tx,k} \times G_{rx,k} \times G_{ijk}, \tag{13}$$

where, the variables $P_{tx,k}$, $G_{tx,k}$, and $G_{rx,k}$ represent the transmit power, the transmitter antenna gains, and antenna gains of the receiver at t_k respectively. The channel gain includes factors such as path loss and fading.

The SNR for the link between GW_i and the corresponding S_j at t_k is determined by using the received power relative to the noise. It is represented as

$$SNR_{ij}(t_k) = \frac{P_{rx,ij}(t_k)}{N_0 \times B}, \tag{14}$$

where $P_{rx,ij}(t_k)$ is the received power for GW_i and S_j at t_k, N_0 indicate the noise spectral density, and B represents the bandwidth.

The data rate for each pair of gateway stations and satellite can be calculated using the following formula [38]

$$R_{ij}(t_k) = B \times \log_2\big(1 + SNR_{ij}(t_k)\big). \tag{15}$$

Subsequently, the average data rate can be expressed as follows

$$\overline{R}(t_k) = \frac{1}{M}\sum_{i=1}^{M} R_{ij}(t_k), \tag{16}$$

where M signifies the total number of active gateway stations at time k.

B. STRATEGY COST

Evaluating handover cost is crucial in satellite network operations, particularly for large constellations like Starlink. This metric analyzes the operational efficiency and economic impacts of handover strategies. It is important to note that the handover cost does not solely depend on reducing the number of handover occurrences [44], [46]. The cost of a single handover is defined as $\ell + s$, where ℓ is related to the latency and represents the hop distance between the current and the next serving satellite [44]. s is a constant for link setup cost, accounting for signaling and resource allocation overhead [44]. This assumes the new path routes through the current satellite to the new one, which might not always be optimal. This formulation aligns with existing literature, where handover costs are modeled as a combination of dynamic and static components.

The set $\mathcal{H}$ includes all handover events that occur during the simulation time and the total number of handover events denoted by $\mathcal{N}$. Each element, h, within this set, represents a specific handover where a gateway station switches from the serving satellite to the target satellite due to the satellite moving out of coverage or other operational needs. This could be defined as follows

$$\mathcal{H} = \{h | 1 \le h \le \mathcal{N}\}. \tag{17}$$

Based on the methodology presented in [44], the overall handover cost, $\mathcal{C}_H$, for a strategy is the sum of all individual handover costs, calculated as

$$\mathcal{C}_H = \sum_{h \in \text{handovers}} (\ell_h + s), \tag{18}$$

where ℓ_h denotes the hop count for each handover h, and s is a constant representing the setup cost, here assumed to be 10. The hop count specifies the number of satellites data must cross when transferring from the current service satellite to the candidate satellite. Our model assumes that each satellite is equipped with four inter-satellite link (ISL) terminals, which can establish connections within a maximum range of 5000 km.

To analyze the effects of energy consumption, E_h, and round-trip time (RTT) on overall performance, strategy cost, $\mathcal{C}_S$, define as follows

$$\mathcal{C}_S = \sum_{h \in \text{handovers}} ((\ell_h + s) \ + \alpha_1 \cdot E_h + \alpha_2 \cdot RTT_h), \tag{19}$$

where E_h is the energy consumption for the h-th handover, defined as

$$E_h = P_{tx} \cdot t_{ijh}^{trans}, \tag{20}$$

where t_{ijh}^{trans} is the transmission delay between GW_i and S_j, given by

$$t_{ijh}^{trans} = \frac{L}{R_{ijh}}, \tag{21}$$

where L define as the data size and R_{ijh} representing the transmission rate between GW_i and S_j.

The term RTT_h represents the round-trip time for the h-th handover and is expressed as

$$RTT_h = 2 \cdot \frac{d_{ijh}}{c} + T_{\text{processing}}, \tag{22}$$

where d_{ijh} is the propagation distance, c is the speed of light, and $T_{\text{processing}}$ is the processing time at the satellite. The weighting factors α_1 and α_2 are used to scale the impact of energy consumption and RTT, respectively, in the total cost.

V. FRAMEWORK EVALUATION

A. COMPLEXITY ANALYSIS

In this section, we analyze the computational complexity of the proposed scheme and demonstrate that the proposed algorithm leads to a much lower computational complexity than the exhaustive search to find the best handover strategy. For a fair comparison, we consider the worst case of our algorithm which results in maximum complexity.

The proposed algorithm is performed over K time slots, representing the handover decision moments. Therefore, the total computational complexity of the proposed scheme can be expressed as a linear function of the complexity of its main components as follows [45]:

$$\varsigma_T = \mathcal{O}\big(\varsigma_{GW} + K\big(\varsigma_{\mathcal{G}} + \varsigma_{KM}\big)\big), \tag{23}$$

where $\varsigma_{GW} = \mathcal{O}(MN)$ represents the complexity of the initial step, which involves searching for covering satellite information for all M gateway stations and N satellites. $\varsigma_{\mathcal{G}} = \mathcal{O}(MN')$ refers to the complexity of establishing the bipartite graph matrices and adjusting weights based on the HM condition, where N' represents the subset of satellites visible to a gateway station and is approximately $N' = 0.05N$, accounting for the worst-case scenario where only 5% of the total satellites are visible. Finally, $\varsigma_{KM} = \mathcal{O}((N'M)^3)$ corresponds to the computational complexity of the KM algorithm applied to the reduced bipartite graph.

By substituting ς_{GW}, $\varsigma_{\mathcal{G}}$, and ς_{KM} into (23), it can be found that the main computational complexity of proposed algorithm comes from KM. Since $N' = 0.05N$, the complexity of the KM algorithm is significantly reduced compared

TABLE 3. Comparison of computational complexity with existing methods.

Study	Algorithm	Algorithm Complexity	Total Complexity
[39]	Directed Graph, Dijkstra Algorithm	$\mathcal{O}(V^2)$	$\mathcal{O}(MN^2)$
[30]	Multi-Attribute Graph, Genetic Algorithm	$\mathcal{O}(g \cdot n \cdot m)$	$\mathcal{O}(gM^2N)$
[36]	Bipartite Graph, Entropy Method	$\mathcal{O}(M \cdot N)$	$\mathcal{O}(MN^2)$
[14]	Multi Attribute Dynamic Graph, Floyd Algorithm	$\mathcal{O}(V^3)$	$\mathcal{O}((M+N)^3)$
Proposed Scheme	Bipartite Graph, KM Algorithm	$\mathcal{O}((N'M)^3)$	$\mathcal{O}((0.05MN)^3)$

to operating on the full set of N satellites. As a result, the total complexity of the proposed scheme is approximately:

$$\varsigma_T \approx \mathcal{O}\left(\left(N'M\right)^3\right) = \mathcal{O}\left((0.05NM)^3\right). \tag{24}$$

This complexity is much less than the complexity resulting from an exhaustive search for designing handover strategy. The reason is that the computational complexity of the exhaustive search is equal to K in an exponential function obtained by multiplying the number of gateways, M, and the number of satellites, N. Therefore, the exhaustive search solution leads to much higher computational complexity than the proposed algorithm.

To further evaluate the computational efficiency of the proposed method, we compare its complexity with several existing state-of-the-art methods, as summarized in Table 3. The comparison is focused on the main complexity components of each study, considering a single handover decision.

In this table, we define V as the number of vertices in the graph, g as the number of generations in the genetic algorithm, n as the population size, and m as the size of individuals. Generally, N represents the total number of satellites, while M denote as gateway station or user. Unlike many existing methods that do not explicitly state satellite filtering assumptions, we consider that these studies might also implicitly filter visible satellites during processing. However, as their explicit complexities are unavailable in some cases, we focus on their primary algorithmic components to provide a fair comparison.

From the table, it is evident that our proposed scheme significantly reducing the computational burden by applying the KM algorithm only to visible satellites (N'). This results in a complexity of $\mathcal{O}((N'M)^3)$, which is much lower than the exhaustive consideration of all satellites (N) in large-scale networks.

B. SIMULATION SETUP

To evaluate the effectiveness of the proposed method, we compare it with three existing strategies: (i) the MWM strategy [40], which maximize data rate but overlooks frequent handovers; (ii) the graph-based shortest path strategy [39], which consider both link quality (using elevation angle) and handover rates (using service time); and (iii) the MST strategy, which minimizes handover frequency but does not prioritize data rate. Specifically, we aim to show that our method achieves data rates comparable to the MWM strategy and better than the shortest path strategy while maintaining a handover rate and handover cost close to the MST strategy.

TABLE 4. A summary of predefined parameters.

Parameter	Value
Simulation time	45 minutes
Altitude	550 km
Transmit power	400 Watts
Carrier frequency	11.9 GHz
Bandwidth	10 MHz
Noise power spectral density	-173 dBm/Hz
Atmospheric fading's attenuation	0.05 dB/km
Rician K-factor	20 dB
Large value of hysteresis coefficient	10 dB
Data Size	1,000 KB

The proposed handover strategy is simulated using Python within a Starlink Phase I constellation environment. The constellation consists of 1,584 satellites, distributed across 22 orbital planes, with 72 satellites per orbit, at an altitude of 550 km [47]. We consider three gateway stations in Montreal, each covered by multiple satellites at different time slots. The duration of the simulation is 45 minutes. A gateway station is within a satellite's coverage area when the elevation angle is 15° or higher. The system settings have been determined in accordance with the works and recommendations in [5] and the implementation trends of the LEO satellite [49].

Table 4 provides a summary of the predefined parameters for simulation.

In this simulation, the HM condition is based on the dynamic channel gain G'_{ij} between GW_i and S_j, which is calculated at the initial matching between each gateway station and satellite. The HM is applied to ensure that as long as the current channel gain between GW_i and S_j does not fall below G'_{ij} by more than the HM value, the satellite connection is maintained. This adaptive approach eliminates the need for a fixed minimum signal threshold (such as reference signal received power (RSRP)) and allows the system to dynamically adjust based on real-time channel conditions.

C. RESULTS AND DISCUSSION

Fig. 5 demonstrates the performance of the proposed strategy under varying HM values. The HM setting is crucial in balancing between reducing handovers and maintaining high data rates. As the HM increases, the average data rate generally declines. Lower margins, such as 2 dB and 3 dB, maintain relatively high data rates and stable performance,

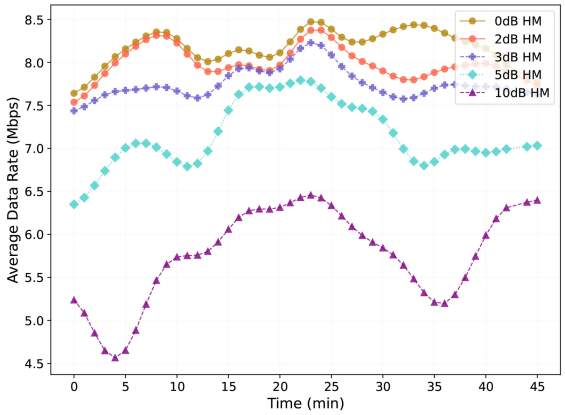

FIGURE 5. Average data rate across different HMs.

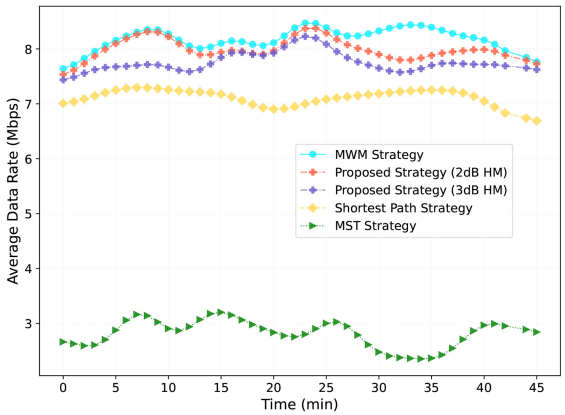

FIGURE 6. Average data rate of handover strategies.

indicating a balance between service continuity and channel quality, making them suitable for environments where high data rates are prioritized. Moderate margins, like 5 dB, effectively balance reduced handover frequency with a slight drop in data rate, highlighting their potential for minimizing handover costs. Higher margins, such as 10 dB, result in further declines in data rate and greater fluctuations, indicating reduced service quality and a dominant role of HM over the KM algorithm in the handover process. These higher thresholds are less ideal for scenarios requiring stable, high-quality connections.

Fig. 6 represents the average data rates for four strategies: the proposed handover strategy, the MWM strategy from [40], the shortest handover path strategy from [39], and the MST strategy. The MWM strategy achieves competitive data rates but overlooks frequent handover, risking service interruptions and user experience degradation. The proposed strategy, incorporating 2 dB and 3 dB margins, effectively balances link quality and handover frequency. As shown, the average data rate of our scheme, especially with the 2 dB margin, closely matches that of the MWM strategy and managing handovers effectively without sacrificing performance. Additionally, it offers robust network stability and high QoS. The proposed scheme with both margins

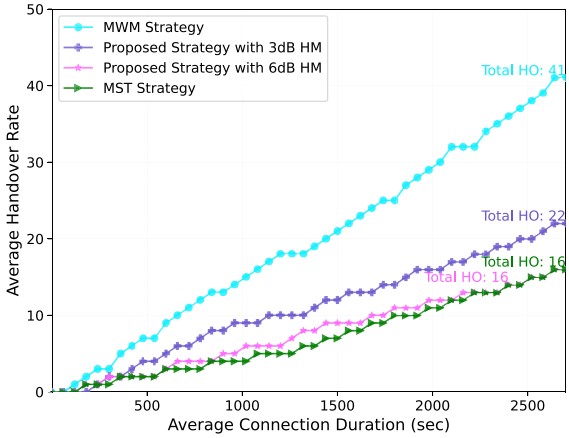

FIGURE 7. Comparison of handover rate across three techniques.

consistently outperforms the shortest path strategy in data rates, demonstrating its ability to leverage satellite diversity and dynamic handover thresholds. In contrast, the MST strategy results in lower data rates, illustrating the challenge of balancing reduced handover numbers with maintaining high data rates.

Fig. 7 shows that the number of handover times increases approximately linearly with the increase of connection duration across three different approaches. By examining these strategies, it has been shown the MST approach shows the slowest increase in the number of handover, while the MWM approach experiences the quickest increase. The handover number of our proposed method, with 3 dB and 6 dB margins, increase at a rate between those approaches and remaining close to the service time approach. It can also be found that the 6 dB margin aligns closely with the number of switches in the MST strategy. The 3 dB margin significantly reduces the number of handovers and improves service continuity while providing a high service quality comparable to the MWM approach. The 3 dB margin is ideal for environments where both high service quality and low handover frequency are essential. Meanwhile, the 6 dB margin suits scenarios prioritizing continuous service over peak service performance. The number of handovers is critical for users and systems as it directly impacts the QoE and the system's signaling overhead. Frequent handovers can lead to increased connection drops, signaling interactions, operational costs, and waste system resources.

Fig. 8 demonstrates that increasing the HM reduces the number of handovers within the network. The optimal margins (i.e., 2 dB and 3 dB) of our proposed method significantly reduce handovers by 45% to 50% compared to 0 dB margin, while preserving comparable communication quality. It displays their performance to achieve the perfect balance between QoS and operational efficiency. Moreover, utilization of 5 dB to 7 dB margins further reduces handovers by 25% to 27% compared to the 2 dB and 3 dB margins. However, this setting is accompanied by a minor degradation in link quality and should be

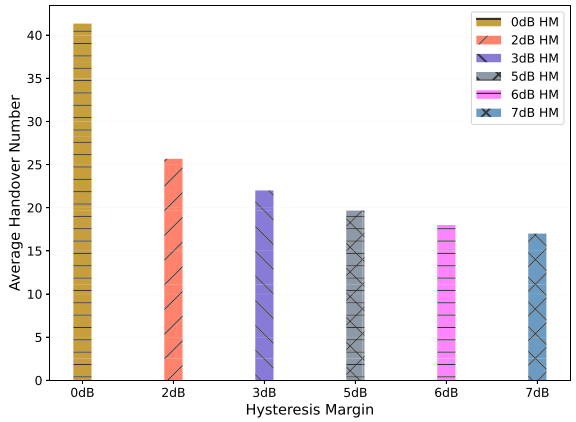

FIGURE 8. Average handover numbers vs different margins.

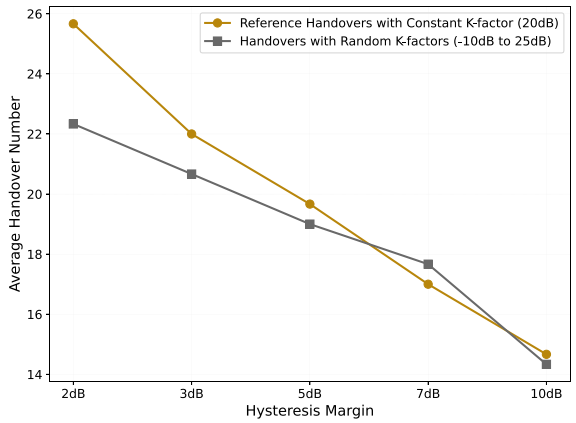

FIGURE 9. Average handover number vs margins.

applied cautiously where high data rates are crucial. This analysis highlights the importance of selecting an appropriate HM to minimize handover events while maintaining high-quality communication in dynamic satellite communication environments.

Fig. 9 evaluates the impact of varying Rician K-factors, uniformly distributed on a linear scale between -10 dB and 25 dB, compared to a constant K-factor baseline of 20 dB. The results show a decrease in handover rates as HM increases across both scenarios. However, under random K-factors, the reduction in handover rates is more pronounced at lower margins, such as 2 dB and 3 dB. This behavior is attributed to dynamic improvements in link quality. In real-world scenarios, satellite movement and changing geometrical configurations can temporarily boost the K-factor, enhancing link quality in subsequent time slots. At lower margins, the algorithm adapts effectively to these signal improvements, maintaining connections with the current satellite and avoiding unnecessary handovers. At higher margins, this adaptability becomes less impactful as the strict HM thresholds inherently reduce handovers regardless of signal fluctuations.

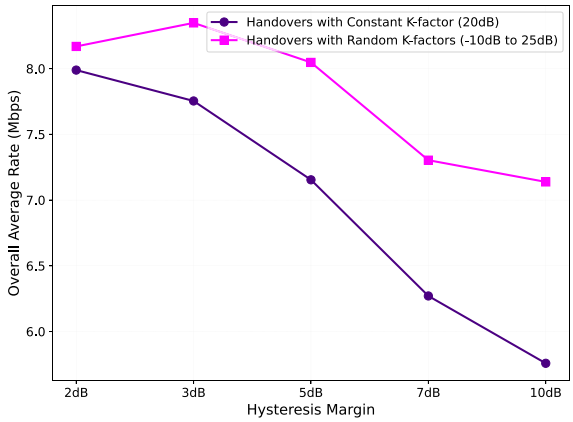

FIGURE 10. Overall average data rates vs HMs.

Fig. 10 compares the overall average data rates for the constant and random K-factor scenarios across different HM values. The results indicate that the random K-factor scenario generally achieves higher data rates, particularly at higher margins such as 5 dB and 7 dB. This improvement stems from the algorithm's ability to capitalize on favorable signal conditions. When the K-factor dynamically increases, link quality improves, enabling the algorithm to maintain connections with high-quality satellites for extended durations, especially at higher margins. In contrast, at lower margins like 2 dB, the KM algorithm prioritizes selecting highest-quality links and plays a dominant role in handover decisions, which limits the visible impact of variable K-factors on the average data rate.

The findings from Fig. 9 and Fig. 10 demonstrate the proposed algorithm's robustness in adapting to dynamic signal conditions, effectively balancing reduced handover frequency with service continuity and enhanced QoS. This adaptability is crucial for improving network efficiency, minimizing signaling overhead, and optimizing resource utilization in real-world satellite communication environments. The results indicate that HM settings could be adjusted and optimized based on specific operational requirements. Lower margins, such as 3 dB, are particularly effective for scenarios prioritizing high service quality and reduced handover rates, offering a balance between continuity and user experience. The proposed approach ensures consistent, high-quality communication and robust performance in dynamic network conditions.

Fig. 11 shows the handover costs for three strategies in a LEO satellite network: the MWM strategy, our proposed strategy (KMHM), and the MST strategy. The ratios β and δ represent the proposed strategy's and the MWM strategies' handover cost relative to the MST strategy, and they are defined as follows

$$\delta = (\text{handover cost of MWM})/(\text{handover cost of MST})$$
$$\beta = (\text{handover cost of KMHM})/(\text{handover cost of MST}).$$

In this regard, Fig. 11 shows significant variations in handover cost among the strategies. The MWM strategy, α,

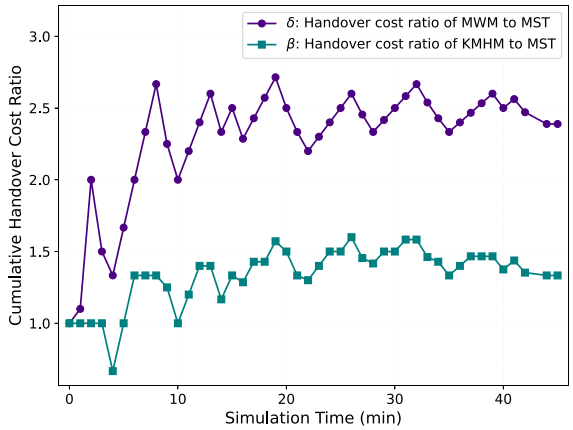

FIGURE 11. Handover cost ratios vs simulation time.

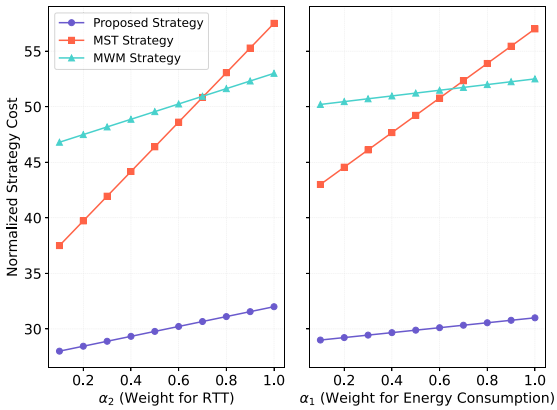

FIGURE 12. Cost value comparison for different strategies.

consistently has a ratio much greater than 1, indicating higher costs due to frequent handovers. In contrast, the proposed KMHM strategy, β, remains closer to 1, indicating an effective reduction in handover cost. Therefore, the proposed scheme, especially with the 3 dB margin, reduces operational costs and unnecessary handover through strategic delays in handover decisions. Moreover, the flexibility of the proposed strategy with adjustable HM allows for further improvement based on specific network requirements. By accurately adjusting the margin, network operators can balance reducing frequent handover and costs while improving link quality.

Fig. 12 illustrates the impact of energy consumption weight (α_1) and RTT weight (α_2) on the normalized strategy cost for the proposed strategy, MST strategy, and MWM strategy. The MST strategy shows the steepest increase in cost for both α_1 and α_2, indicating its high sensitivity to latency and energy consumption due to its strict handover minimization. The MWM strategy exhibits a more moderate slope but starts with higher costs, reflecting its focus on maximizing data rates without addressing frequent handovers. In contrast, the proposed strategy with 3 dB margin remains less sensitive to variations in both weights, maintaining a consistently lower cost profile. This

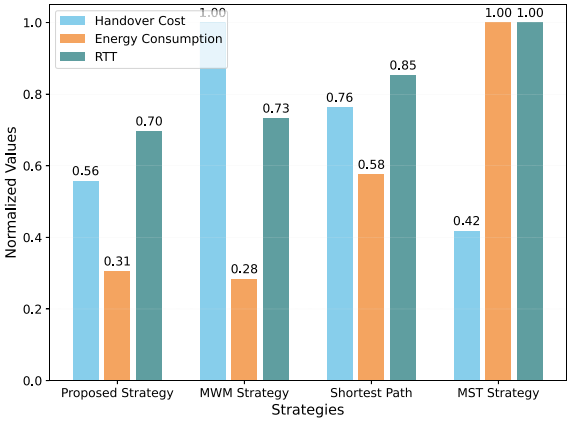

FIGURE 13. Normalized performance comparison across strategies.

demonstrates the proposed strategy's robustness and ability to balance performance across varying latency and energy conditions.

Fig. 13 compares the normalized handover cost, energy consumption, and RTT across four strategies. The proposed strategy achieves the lowest RTT, indicating its effectiveness in minimizing communication delay, which is crucial for latency-sensitive applications. It also significantly reduces the handover cost compared to MWM and the shortest path strategy, while being slightly higher than MST, which prioritizes stability at the expense of data rate. For energy consumption, the proposed strategy remains close to MWM, which maximizes data rate but incurs higher handover frequency. This highlights the potential of the proposed strategy to achieve comparable energy efficiency with further HM optimization. Overall, the proposed strategy balances all three metrics effectively, reducing handover costs and latency while maintaining competitive energy consumption.

VI. CONCLUSION

In this paper, we proposed a handover strategy for LEO satellite networks based on a bipartite graph model, aiming to maximize the overall communication quality, minimize the handover rate, and balance the network load. Furthermore, we introduced a novel integration of HM with KM algorithm, which provides a flexible, robust, and adaptable framework to meet different network requirements. The provided simulation results show that the average data rate of the proposed scheme closely matches the MWM strategy while outperforming the shortest handover path strategy. In addition, our scheme significantly reduces the handover rate and handover costs, and communication latency, while achieving energy consumption levels comparable to the MWM strategy. These improvements highlight the proposed strategy's ability to deliver stable, efficient, and low-latency communication. Future investigations should implement multi-connectivity in the satellite handover strategy to fully utilize satellite resources and improve data rates. Moreover, exploring

multi-objective optimization techniques, such as optimizing data rates, handover frequency, and energy efficiency simultaneously, would help in effectively balancing system performance metrics. Pareto front analysis could identify the best configurations to balance these conflicting objectives. Moreover, developing dynamic, re-configurable HM settings based on real-time network conditions through advanced technologies such as machine learning can further enhance the handover strategy and adapt it to varying operational environments.

REFERENCES

[1] T. Darwish, G. K. Kurt, H. Yanikomeroglu, M. Bellemare, and G. Lamontagne, "LEO satellites in 5G and beyond networks: A review from a standardization perspective," *IEEE Access*, vol. 10, pp. 35040–35060, 2022.

[2] S. Kota and G. Giambene, "6G integrated non-terrestrial networks: Emerging technologies and challenges," in *Proc. IEEE Int. Conf. Commun. Workshops*, Jun. 2021, pp. 1–6.

[3] G. Araniti, A. Iera, S. Pizzi, and F. Rinaldi, "Toward 6G non-terrestrial networks," *IEEE Netw.*, vol. 36, no. 1, pp. 113–120, Jan./Feb. 2022.

[4] D. Zhou, M. Sheng, J. Li, and Z. Han, "Aerospace integrated networks innovation for empowering 6G: A survey and future challenges," *IEEE Commun. Surveys Tuts.*, vol. 25, no. 2, pp. 975–1019, 2nd Quart., 2023.

[5] "Solutions for NR to support non-terrestrial networks (NTN), (Release 16)," 3GPP, Sophia Antipolis, France, Rep. 38.821, May 2021.

[6] A. Tuysuz and F. Alagoz, "Satellite mobility pattern based handover management algorithm in LEO satellites," in *Proc. IEEE Int. Conf. Commun.*, 2006, pp. 1867–1872.

[7] J. Wang, W. Mu, Y. Liu, L. Guo, S. Zhang, and G. Gui, "Deep reinforcement learning-based satellite handover scheme for satellite communications," in *Proc. Int. Conf. Wireless Commun. Signal Process. (WCSP)*, 2021, pp. 1–6.

[8] S. L. Kota, K. Pahlavan, and P. Leppanen, *Broadband Satellite Communications for Internet Access*. Hingham, MA, USA: Kluwer Academic Publ., 2004.

[9] E. Juan, M. Lauridsen, J. Wigard, and P. Mogensen, "Handover solutions for 5G low-earth orbit satellite networks," *IEEE Access*, vol. 10, pp. 93309–93325, 2022.

[10] F. Wang, D. Jiang, Z. Wang, J. Chen, and T. Q. S. Quek, "Seamless handover in LEO Based non-terrestrial networks: Service continuity and optimization," *IEEE Trans. Commun.*, vol. 71, no. 2, pp. 1008–1023, Feb. 2023.

[11] W. Lin et al., "A novel method to determine the handover threshold based on reconfigurable factor graph for LEO satellite Internet network," *IEEE Access*, vol. 10, pp. 31907–31921, 2022.

[12] M. Y. Abdelsadek, G. K. Kurt, and H. Yanikomeroglu, "Distributed massive MIMO for LEO satellite networks," *IEEE Open J. Commun. Soc.*, vol. 3, pp. 2162–2177, 2022.

[13] A. M. Voicu, A. Bhattacharya, and M. Petrova, "Handover strategies for emerging LEO, MEO, and HEO satellite networks," *IEEE Access*, vol. 12, pp. 31523–31537, 2024.

[14] C.-Q. Dai, Y. Liu, S. Fu, J. Wu, and Q. Chen, "Dynamic handover in satellite-terrestrial integrated networks," in *Proc. IEEE Global Commun. Conf. Workshops (Globecom Workshops)*, Dec. 2019, pp. 1–6.

[15] E. Papapetrou, S. Karapantazis, and G. Dimitriadis, "Satellite handover techniques for LEO networks," *Int. J. Satell. Commun. Netw.*, vol. 22, no. 2, pp. 231–245, 2010.

[16] X. Hu, H. Song, S. Liu, and W. Wang, "Velocity-aware handover prediction in LEO satellite communication networks," *Int. J. Satell. Commun. Netw.*, vol. 36, no. 6, pp. 451–459, May 2018.

[17] H. Xu, D. Li, M. Liu, G. Han, W. Huang, and C. Xu, "QoE-driven intelligent handover for user-centric mobile satellite networks," *IEEE Trans. Veh. Technol.*, vol. 69, no. 9, pp. 10127–10139, Sep. 2020.

[18] T. Leng, Y. Xu, G. Cui, and W. Wang, "Caching-aware intelligent handover strategy for LEO satellite networks," *Remote Sens.*, vol. 13, no. 11, p. 2230, 2021.

[19] J. Miao, P. Wang, H. Yin, N. Chen, and X. Wang, "A multi-attribute decision handover scheme for LEO mobile satellite networks," in *Proc. IEEE Int. Conf. Commun. China (ICCC)*, Dec. 2019, pp. 938–942.

[20] I. Shayea et al., "New weight function for adapting handover margin level over contiguous carrier aggregation deployment scenarios in LTE-advanced system," *Wireless Pers. Commun.*, vol. 108, no. 2, pp. 1179–1199, 2019.

[21] W. Zhaofeng, H. Guyu, Y. Seyedi, and J. Fenglin, "A simple real-time handover management in the mobile satellite communication networks," in *Proc. Asia-Pacific Netw. Oper. Manag. Symp.*, 2015, pp. 175–179.

[22] Y. Li, W. Zhou, and S. Zhou, "Forecast based handover in an extensible multi-layer LEO mobile satellite system," *IEEE Access*, vol. 8, pp. 42768–42783, 2020.

[23] S. He, T. Wang, and S. Wang, "Load-aware satellite handover strategy based on multi-agent reinforcement learning," in *Proc. IEEE Global Commun. Conf. (GLOBECOM)*, Dec. 2020, pp. 1–6.

[24] J. Li, K. Xue, J. Liu, and Y. Zhang, "A user-centric handover scheme for ultra-dense LEO satellite networks," *IEEE Wireless Commun. Lett.*, vol. 9, no. 11, pp. 1904–1908, Nov. 2020.

[25] B. Yang, Y. Wu, X. Chu, and G. Song, "Seamless handover in software-defined satellite networking," *IEEE Commun. Lett.*, vol. 20, no. 9, pp. 1768–1771, Sep. 2016.

[26] K. Xue, W. Meng, S. Li, D. S. L. Wei, H. Zhou, and N. Yu, "A secure and efficient access and handover authentication protocol for Internet of Things in space information networks," *IEEE Internet Things J.*, vol. 6, no. 3, pp. 5485–5499, Jun. 2019.

[27] C. Duan, J. Feng, H. Chang, B. Song, and Z. Xu, "A novel handover control strategy combined with multi-hop routing in LEO satellite networks," in *Proc. IEEE Int. Parallel Distrib. Process. Symp. Workshops*, 2018, pp. 845–851.

[28] Y. Cao, S.-Y. Lien, and Y.-C. Liang, "Deep reinforcement learning for multi-user access control in non-terrestrial networks," *IEEE Trans. Commun.*, vol. 69, no. 3, pp. 1605–1619, Mar. 2021.

[29] G. Maral, J. Restrepo, E. del Re, R. Fantacci, and G. Giambene, "Performance analysis for a guaranteed handover service in an LEO constellation with a 'satellite-fixed cell' system," *IEEE Trans. Veh. Technol.*, vol. 47, no. 4, pp. 1200–1214, Nov. 1998.

[30] H. Li, R. Liu, B. Hu, L. Ni, and C. Wang, "A multi-attribute graph based handover scheme for LEO satellite communication networks," in *Proc. Int. Conf. Comput. Sci. Netw. Technol. (ICCSNT)*, 2022, pp. 127–131.

[31] K. Xue, W. Meng, H. Zhou, D. S. L. Wei, and M. Guizani, "A lightweight and secure group key based handover authentication protocol for the software-defined space information network," *IEEE Trans. Wireless Commun.*, vol. 19, no. 6, pp. 3673–3684, Jun. 2020.

[32] P. K. Chowdhury, M. Atiquzzaman, and W. Ivancic, "Handover schemes in satellite networks: State-of-the-art and future research directions," *IEEE Commun. Surveys Tuts.*, vol. 8, no. 4, pp. 2–14, 4th Quart., 2006.

[33] Y. Liu et al., "Joint optimization based satellite handover strategy for low earth orbit satellite networks," *IET Commun.*, vol. 15, pp. 1576–1585, Mar. 2021.

[34] Z. Xiao, J. Yang, T. Mao, C. Xu, R.-Z. Han, and X.-G. Xia, "LEO satellite access network (LEO-SAN) Towards 6G: Challenges and approaches," 2022, *arXiv:2207.11896*.

[35] A. Bottcher and R. Werner, "Strategies for handover control in low earth orbit satellite systems," in *Proc. IEEE Veh. Technol. Conf. (VTC)*, 1994, pp. 1616–1620.

[36] S. Zhang, A. Liu, and X. Liang, "A multi-objective satellite handover strategy based on entropy in LEO satellite communications," in *Proc. Int. Conf. Comput. Commun. (ICCC)*, 2020, pp. 723–728.

[37] M. Hozayen, T. Darwish, G. K. Kurt, and H. Yanikomeroglu, "A graph-based customizable handover framework for LEO satellite networks," in *Proc. IEEE Globecom Workshops (GC Wkshps)*, 2022, pp. 868–873.

[38] M. Hosseini, R. Ghazizadeh, and H. Farhadi, "Game theory-based radio resource allocation in NOMA vehicular communication networks supported by UAV," *Phys. Commun.*, vol. 52, Jun. 2022, Art. no. 101681.
[39] Z. Wu, F. Jin, J. Luo, Y. Fu, J. Shan, and G. Hu, "A graph-based satellite handover framework for LEO satellite communication networks," *IEEE Commun. Lett.*, vol. 20, no. 8, pp. 1547–1550, Aug. 2016.
[40] L. Feng, Y. Liu, L. Wu, Z. Zhang, and J. Dang, "A satellite handover strategy based on MIMO technology in LEO satellite networks," *IEEE Commun. Lett.*, vol. 24, no. 7, pp. 1505–1509, Jul. 2020.
[41] I. Ali, N. Al-Dhahir, and J. E. Hershey, "Predicting the visibility of LEO satellites," *IEEE Trans. Aerosp. Electron. Syst.*, vol. 35, no. 4, pp. 1183–1190, Oct. 1999.
[42] Y. Wu, G. Hu, F. Jin, and J. Zu, "A satellite handover strategy based on the potential game in LEO satellite networks," *IEEE Access*, vol. 7, pp. 133641–133652, 2019.
[43] A. Ibrahim and A. S. Alfa, "Using lagrangian relaxation for radio resource allocation in high altitude platforms," *IEEE Trans. Wireless Commun.*, vol. 14, no. 10, pp. 5823–5835, Oct. 2015.
[44] V. M. Grant, "Proliferated low earth orbit (pLEO) satellite constellation handover cost analysis," M.S. thesis, Dept. Electr. Eng. Comput. Sci., Massachusetts Inst. Technol., Cambridge, MA, USA, Jun. 2023.
[45] M. Hosseini and R. Ghazizadeh, "Stackelberg game-based deployment design and radio resource allocation in coordinated UAVs-assisted vehicular communication networks," *IEEE Trans. Veh. Technol.*, vol. 72, no. 1, pp. 1196–1210, Jan. 2023.
[46] K. Maity, S. Das, A. Saha, B. Pal, and A. Sarkar, "Cost analysis of handover manager based handover method in LEO satellite networks," *IOSR J. Comput. Eng.*, vol. 9, no. 5, pp. 44–51, 2013.
[47] *SpaceX Non-Geostationary Satellite System Attachment A Technical Information to Supplement Schedule S*, SpaceX, Hawthorne, CA, USA, Nov. 2018.
[48] M. Y. Abdelsadek, G. Karabulut-Kurt, H. Yanikomeroglu, P. Hu, G. Lamontagne, and K. Ahmed, "Broadband connectivity for handheld devices via LEO satellites: Is distributed massive MIMO the answer?" *IEEE Open J. Commun. Soc.*, vol. 4, pp. 713–726, 2023.
[49] L. Tian, N. Huot, O. Chef, and J. Famaey, "Self-organising LEO small satellite constellation for 5G MTC and IoT applications," in *Proc. Int. Conf. Netw. Future (NoF)*, 2020, pp. 100–104.
[50] J. Chen, M. Ozger, and C. Cavdar, "Nash soft actor-critic LEO satellite handover management algorithm for flying vehicles," in *Proc. IEEE Int. Conf. Mach. Learn. Commun. Netw. (ICMLCN)*, 2024, pp. 380–385.
[51] J. Liang et al., "Latency versus transmission power trade-off in free-space optical (FSO) satellite networks with multiple inter-continental connections," *IEEE Open J. Commun. Soc.*, vol. 4, pp. 3014–3029, 2023.

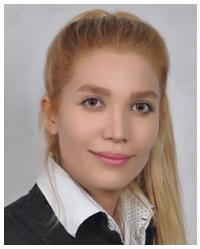

SAHAR EYDIAN received the B.S. degree in electronics and electrical engineering from Dr. Shariaty University, Tehran, Iran, in 2016, and the M.A.Sc. degree in electrical engineering from Polytechnique Montréal, Montréal, Canada, in 2024. She gained experience in terrestrial wireless communications, including implementing new technologies in 5G and 4G in various companies, such as Huawei and Ericsson, from 2016 to 2021. In 2021, she established Ctech Communications Company and held the position of CEO. Her research interests include satellite communications, space networks, space security, and machine learning applications.

MARYAM HOSSEINI received the Ph.D. degree in electrical engineering from the University of Birjand, Birjand, Iran, in 2022. She is a Postdoctoral Research Fellow with Polytechnique Montréal, Montréal, Canada. She also joined as a Visiting Researcher and worked on brain communication modeling with the KTH Royal Institute of Technology, Stockholm, Sweden, from 2019 to 2020. Her research interests mainly focus on game theory and machine learning for a broad range of applications including wireless communications, wireless healthcare systems, vehicular networks, and satellite communications.

GUNES KARABULUT KURT (Senior Member, IEEE) received the B.S. (Hons.) degree in electronics and electrical engineering from Bogazici University, Istanbul, Türkiye, in 2000, and the M.A.Sc. and Ph.D. degrees in electrical engineering from the University of Ottawa, ON, Canada, in 2002 and 2006, respectively. She is a Canada Research Chair (Tier 1) in New Frontiers in Space Communications and a Professor with Polytechnique Montréal, Montréal, QC, Canada, where she is the Director of the Poly-Grames Research Center, and a Co-Founder and the Director of Education and Training of ASTROLITH, Transdisciplinary Research Unit of Space Resource and Infrastructure Engineering. She is also an Adjunct Research Professor with Carleton University, Canada. She worked in different technology companies in Canada, Türkiye, from 2005 to 2010. From 2010 to 2021, she was a Professor with Istanbul Technical University. She has received the Turkish Academy of Sciences Outstanding Young Scientist (TÜBA-GEBIP) Award in 2019. She is a Marie Curie Fellow.